Exploration of a Metastable Normal Spinel Phase Diagram for the Quaternary Li-Ni-Mn-Co-O System

Wang Hay Kan,[†] Ashfia Huq,[‡] and Arumugam Manthiram^{*,†}

[†]Materials Science and Engineering Program & Texas Materials Institute, The University of Texas at Austin, Austin, Texas 78712, United States

[‡]Neutron Scattering Science Division, Oak Ridge National Laboratory, Oak Ridge, Tennessee 37831, United States

ABSTRACT: In an attempt to enlarge the normal spinel phase diagram for the quaternary Li-Ni-Mn-Co-O system, the transformation at moderate temperatures (150-210 $^{\circ}$ C) of layered Li_{0.5}(Ni_{1-y-z}Mn_yCo_z)O₂ (*R-3m*), which were obtained by an ambient-temperature extraction of lithium from Li_{0.5}(Ni_{1-y-z}Mn_yCo_z)O₂, into normal spinel-like (*Fd-3m*) Li(Ni_{1-y-z}Mn_yCo_z)₂O₄ has been investigated. The phase-conversion mechanism has been studied by a joint time-of-flight (TOF) neutron and X-ray diffractions, thermogravimetric analysis, and bond valence sum map. The ionic diffusion of lithium (*3a*, *6c*) and nickel (*3a*, *3b*) ions has been quantified as a function of temperature. The investigated spinel phases are metastable and they are subject to change into rock-salt phases at higher temperatures. The phases have been characterized as cathodes in lithium-ion cells. The study may serve as a strategic model to access other metastable phases by low-temperature synthesis approaches.

1. INTRODUCTION

Lithium-ion batteries have become the dominant energy-storage technology for portable electronics, electric vehicles, and stationary storage of electrical energy generated from renewable energy sources. Since the conventional cathodes (*e.g.*, LiCoO₂ and LiMn₂O₄) developed in the 1980s by Goodenough's group, ¹⁻³ a large number of new cathodes have been explored in the last two decades aiming to achieve better specific capacity, power capability, thermal/chemical stability, and durability. ⁴⁻⁶ Notably, LiFePO₄ is one of the most promising polyanion-based cathodes as it shows excellent thermal stability and cycling ability, although its electrical and ionic conductivities are intrinsically low. ⁷⁻⁸

For automotive applications, lithium manganese oxide LiMn₂O₄ with the normal spinel structure has been widely considered as a major component for cathode because of its low cost, low toxicity, high cell voltage, high tap density, and high rate capability. 9-11 After the first report on the pristine LiMn₂O₄ in 1983, some new members have been synthesized by partially substituting other ions for Mn as in LiMn_{2-v}M_vO₄ (M = Li, Mg, Ti, V, Cr, Fe, Co, Ni, and Zn). 12-14 The use of a low-valent and inert dopant, e.g., Li_{1+x}Mn_{2-x}O₄, has been found to be useful to improve the long-term cycling performance by rising the valence of Mn^{n+} ions to >3.5+ and thereby reducing the cooperative Jahn-Teller effect.¹⁴ Another fascinating composition is LiMn_{1.5}Ni_{0.5}O₄ as the small amount of substitution (up to 25 %) of nickel ions can alter the entire redox chemistry from Mn^{3+/4+} into Ni^{2+/4+} during electrochemical cycling.¹⁵ Its practical application is, however, yet to be fully evaluated due to the lack of suitable electrolytes at the high operating voltage of ~ 4.7 V.⁶

Co-doping (i.e., using more than one-type of dopants) is widely adopted strategy as it can help to optimize the chemi-

cal/physical properties of a system that a single dopant might not be able to. One of the most known examples is the layered LiNi_{1/3}Mn_{1/3}Co_{1/3}O₂, which exhibits superior electrochemical performance in term of practical specific capacity, thermal stability, and cyclability, as compared to LiNi_{1-y}Co_yO₂ and LiNi_{1-y}Mn_yO₂. ¹⁶⁻²⁰ ~ 80 or so layered-type (O3) compounds with different compositions for the quaternary Li-Ni-Mn-Co-O system have been reported over the years. ²¹ But quite surprisingly, no known compounds with the normal spinel-type structure for the same quaternary system are found in the International Compounds for Diffraction Data (ICDD). ²¹ Recently, Brown *et al.* studied the Li-Ni-Mn-Co-O system using combinatorial co-precipitation method hoping to identify new crystal phases. ²² They confirmed that the normal spinels could not be made by conventional solid-state method.

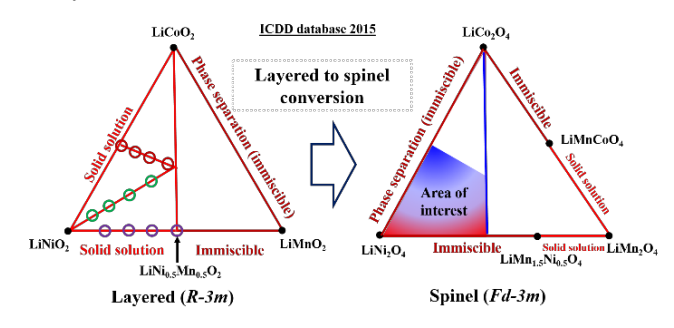


Figure 1. Schematic diagram showing that some metastable normal spinels could be prepared from their layered-type analogs in the Li-Ni-Mn-Co-O system.

Not long ago, Shukla *et al.* observed the presence of a Nirich spinel phase on the surface of Li_{1.2}(Ni_{0.13}Mn_{0.54}Co_{0.13})O₂ crystals by high-resolution electron microscopy and spectroscopy techniques.²³ This finding encouraged us to look for oth-

er metastable spinels and study their physical/chemical properties. One of our recent studies also showed that metastable Nirich spinels with a general chemical formula LiNi_{2-x}Mn_xO₄ (x = 0.4 to 1) could indeed be prepared by a low-temperature synthesis. Those reports shed some lights on the possibility of preparing new metastable normal spinel members by mild synthetic approaches, *e.g.*, low-temperature phase conversion reactions. Accordingly, we aim to explore in this paper some new metastable spinels, which could exist in the Li-Ni-Mn-Co-O system (Figure 1), via a low-temperature synthesis approach. This could provide a new strategy to access metastable phases by low-temperature-driven conversion reactions.

2. EXPERIMENTAL SECTION

2.1 Synthesis. The layered-type $LiNi_{1-2v}Mn_vCo_vO_2$ (y = 0.1, 0.15, 0.2, and 0.25), $LiNi_{1-2y}Mn_yCo_yO_2$ (y = 0.1, 0.15, 0.2, and 0.25), and LiNi_{0.5-y}Mn_{2y}Co_{0.5-y}O₂ (y = 0, 0.05, 0.1, and 0.15) were prepared by a sol-gel method. Stoichiometric amounts Li(OAc)·2H₂O, $Ni(OAc)_2 \cdot 4H_2O$, Mn(OAc)₂·4H₂O, and Co(OAc)₂·4H₂O were dissolved in deionized water. A 3% excess lithium salt was added to compensate the loss of Li due to evaporation at elevated temperatures. Citric acid, equivalent to the sum of lithium and transition-metal ions, was added to the above solutionas a chelating agent. The solution was first stirred for 30 min at 25 °C and thereafter maintained at 90 °C to form a sol/gel. The dried mixtures were then decomposed at 450 °C, hand-ground, and further heat treated at 800 °C in air for 12 h. The partially delthiated samples Li_{0.5}MO₂ (M = Ni, Mn, and Co) were obtained by reacting the prepared layered oxides with certain amount of NO₂BF₄ in dried acetonitrile under Ar atm for 12 h. The cationic ratios in the samples were verified by inductively coupled plasma atomic emission spectroscopy (ICP-AES).

2.2 Phase characterization. All the samples prepared were first characterized for phase purity by powder X-ray diffraction (PXRD, Rigaku Ultima IV powder x-ray diffractometer, Cu K_a radiation, 40 kV, 44 mA) at $2\theta = 10^{\circ}$ to 80° at a count rate of 10 s per step of 0.02° at room temperature. Synchrotron X-ray diffraction was also performed at ambient temperature at $2\theta = 0.5^{\circ}$ to 50° with a 2θ step size of 0.0001° with a monochromatic X-ray ($\lambda = 0.414 \text{ Å}$) at the Advanced Photon Source (APS), for Li_{0.5}Ni_{0.45}Mn_{0.1}Co_{0.45}O₂ (25, 150, 170, 190, 210 °C) and $Li_{0.5}Ni_{0.35}Mn_{0.3}Co_{0.35}O_2$ (25, 150, 170, 190, 210 °C). The samples were packed into Kapton® Capillary Tubes. Time-of-flight neutron diffraction (ND) data were collected at the Oak Ridge National Laboratory (ORNL) Spallation Neutron Source (SNS) POWGEN beamline using a beam of neutron with a center wavelength of 1.333 Å (covering a dspacing range of 0.4 to 5.4 Å). For in-situ measurements, the samples were packed into a vanadium tube and the data were collected between 25 and 350 °C in a vacuum cryofurnace. For ex-situ measurements, the partially delithated samples were heated between 150 and 210 °C for 12 h in air at the University of Texas at Austin. The samples were then shipped to SNS for ND measurements using vanadium sample tube. For exsitu measurement, the room temperature synchrotron X-ray and neutron datasets were joint-refined by the conventional Rietveld method using the General Structure Analysis System (GSAS) package with the graphical user interface (EXPGUI).²⁵ The background, scale factor, zero (for X-ray only), absorption (for neutron only), cell parameters, atomic positions, thermal parameters and profile coefficients for

Pseudo-Voigt / Finger, Cox, and Jephcoat (FCJ) Asymmetric peak shape function were refined until the convergence was achieved. For *in-situ* measurements, only the neutron diffraction data were used in the refinement. The bond valence sum maps were calculated by 3DBVSMAPPER where the valence of all Mn ions was assumed to be 4+ in all partially delihiated samples. The crystallographic information files (cif) were obtained from International Centre for Diffraction Data (ICDD) database as an imported file for the calculation. Mass change/oxide-ion vacancy was analyzed in air with a NETZSCH Jupiter STA 449 F3 thermogravimetric analyzer.

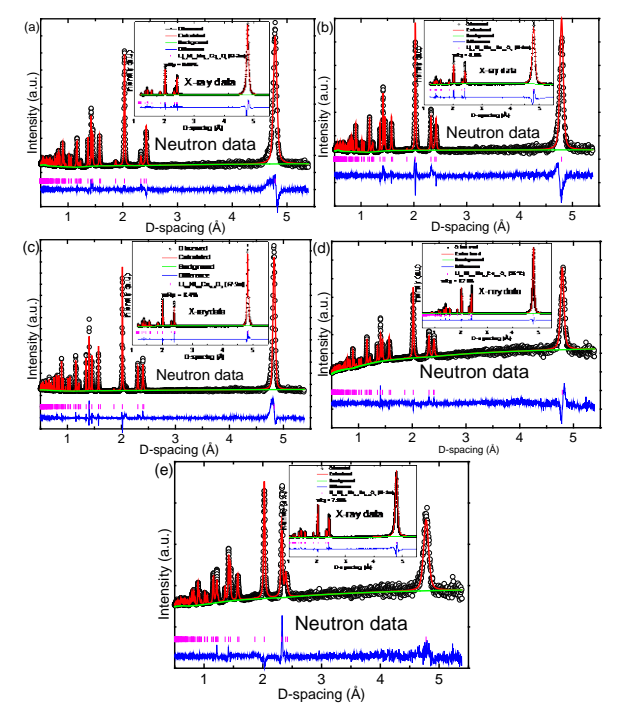
2.3 Electrochemical performance. The electrode-slurry was prepared by simply mixing the active material (80 wt. %), super P (10 wt. %) and polyvinylidene fluoride (PVDF; 10 wt. %) in N-methyl-2-pyrrolidone (NMP) overnight. The slurry was then coated onto an aluminium current collector, dried overnight in a vacuum oven, and used to fabricate the cathode. A CR2032-type coin cell was assembled in an Ar-filled glove box with the cathode thus prepared, 1 M LiPF₆ in ethylene carbonate (EC)/diethyl carbonate (DEC) (1:1 by volume) electrolyte, and metallic lithium anode. The cells were cycled galvanostatically with an Arbin cycler between 2 and 4.9 V at a current rate of 5 mA g⁻¹.

3. RESULTS AND DISCUSSION

3.1 Structural analysis of $LiNi_{1-2v}Mn_vCo_vO_2$ (x = 0.1, 0.15, 0.2, and 0.25) and LiNi_{0.5-v}Mn_{2v}Co_{0.5-v}O₂ (y = 0, 0.05, **0.1, and 0.15).** With an aim to cover the area of interest for the Li-Ni-Mn-Co-O (NMC) system, 8 new NMC layered-type compounds were synthesized, as shown in Figure 1; the other 4 layered compounds $\text{Li}_{0.5} \text{Ni}_{1-y} \text{Mn}_y \text{O}_2$ (y = 0.5 - 0.8) were shown in our earlier report²⁴ that they could transform into spinel-like $\text{LiNi}_{2-y}\text{Mn}_y\text{O}_4$ (y = 0.4 – 1) by a low-temperature synthesis. High purity layered-type samples were prepared by a sol-gel method in which the acetate-based precursors was first dissolved homogeneously into water prior to the heat treatment. The partially delithiated samples were confirmed to maintain their layered-type structure (space group R-3m) by Rietveld refinement on joint neutron and X-ray diffractions (Figure 2 and Table S1). The refinement result also showed that the lithium and transition-metal ions predominantly occupied the 3a and 3b sites, respectively, of the cubic-closepacked oxygen arrays (6c). A small amount of defect, mainly the anti-site defect for Li and Ni ions, was also found, and it was consistent with our previous studies.^{24, 27} The cationic ratio was verified by inductively coupled plasma atomic emission spectroscopy (ICP-AES; Table S2).

The partially delithiated layered-type samples are known for thermal instability and they are subject to change to spinel or rock-salt structures at elevated temperatures. Therefore, the heat treatment temperature range was first determined to avoid any over-heating to yield unwanted rock-salt phases. The formation of rock-salt phase was monitored by thermogravimetric analysis (TGA) and PXRD as a function of temperature. In general, $\text{Li}_{0.5}\text{Ni}_{1-2y}\text{Mn}_y\text{Co}_y\text{O}_2$ (y = 0.1, 0.15, 0.2, and 0.25) were found to have insignificant weight losses of 0.3 - 0.8 wt.% from 25 - 200 °C, as shown in Figure 3a. In other words, 0.9 to 2.2 mol% of oxide-ion vacancy (assuming no adsorbed moisture and residual solvent) were formed in samples below 200 °C, if all the weight losses were used to account for the formation of oxide-ion vacancy (i.e., $2\text{O}^2 \rightarrow \text{O}_2 + 4\text{e}$). Similarly, $\text{Li}_{0.5}\text{Ni}_{0.5-y}\text{Mn}_2\text{vCo}_{0.5-y}\text{O}_2$ (y = 0, 0.05, 0.1,

0.15) were thermally stable, except a larger amount of oxideion vacancy (6.9 mol%) was observed for Li $_{0.5}$ Ni $_{0.5}$ Co $_{0.5}$ O $_{2}$ below 200 °C. From the *ex-situ* PXRD patterns, most of the major peak positions were unchanged, but a progressive merging of (018) and (-120) peaks at $2\theta = 65^{\circ}$ happened from 150 to 200 °C (Figure S1-S8). The relative intensity ratio of (003)/(-114) peak was also found to decrease with increasing temperature, an evidence of the formation rock-salt impurity at the higher temperature regime. However, no other unknown impurities were found for the whole temperature range.



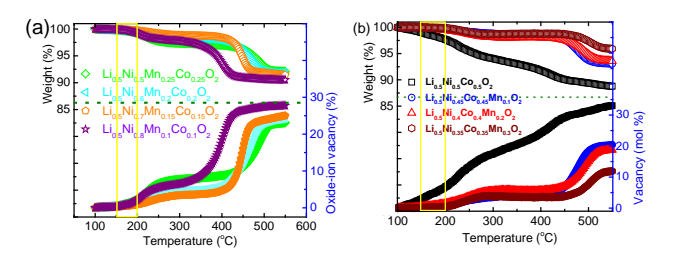


Figure 3. Thermogravimetric analysis of (a) $\text{Li}_{0.5}\text{Ni}_{1-2y}\text{Mn}_y\text{Co}_y\text{O}_2$ (y = 0.1, 0.15, 0.2, and 0.25) and (b) $\text{Li}_{0.5}\text{Ni}_{0.5-y}\text{Mn}_{2y}\text{Co}_{0.5-y}\text{O}_2$ (y = 0, 0.05, 0.1, and 0.15) as a function of temperature. The corresponding oxide-ion vacancy concentration was also calculated.

The detailed phase transformation mechanism was further investigated by time-of-flight (TOF) neutron diffraction. Two nickel rich samples, $\text{Li}_{0.5}\text{Ni}_{0.8}\text{Mn}_{0.1}\text{Co}_{0.1}\text{O}_2$ and $\text{Li}_{0.5}\text{Ni}_{0.6}\text{Mn}_{0.2}\text{Co}_{0.2}\text{O}_2$, were found to be suitable for *in-situ* measurement due to their rapid phase change (within 1 - 2 h). Three other lower nickel-content samples, $\text{Li}_{0.5}\text{Ni}_{0.5}\text{Co}_{0.5}\text{O}_2$, $\text{Li}_{0.5}\text{Ni}_{0.45}\text{Mn}_{0.1}\text{Co}_{0.45}\text{O}_2$, and $\text{Li}_{0.5}\text{Ni}_{0.35}\text{Mn}_{0.3}\text{Co}_{0.35}\text{O}_2$, were studied by *ex-situ* neutron and synchrotron X-ray diffractions

by heat-treating the samples between 150 and 210 $^{\rm o}{\rm C}$ for 12 h prior for each measurement.

Rietveld refinement of the neutron diffraction data was employed to understand the ionic movement of all cations. Various cationic species with similar electron densities or light weight, e.g., Li, Ni, Mn, Co, can be differentiated quantitatively in different crystallographic sites. Two position constrains were created to track all cationic species involved in the transformation reaction: First, all transition-metal ions (3b) were allowed to move into the partially empty octahedral site (3a) for lithium ions. Second, the lithium ions were also allowed to move from their original octahedral 3a sites into an empty tetrahedral 6c site. Most other parameters were allowed to move freely until a convergence was reached.

Among all the cationic species, only lithium and nickel ions were found to move in the layered-type structure between 100 and 210 °C, as shown in Figure 4. The ionic movement of Co and Mn ions were ruled out in the refinement for the entire temperature range, and the kinetic hindrance was not fully understood. The octahedral site stabilization energies (OSSE) were believed to be major factors to govern the diffusion of ionic species, and they were undoubtedly used to explain the transformation of α-NaFeO₂-type LiMnO₂ into spinel-type LiMn₂O₄. ³¹⁻³² However, in our previous study, Mn ions were found to be immobile from 25 - 200 °C in $Li_{0.5}Ni_{1-v}Mn_vO_2$ (y = 0.2 - 0.5), indicating that the electrostatic repulsion could be another critical factor. On the basis of the electronic band structure, the valence state of Mn ions was presumably 4+ due to the lying of $Mn^{3+/4+}$ redox energy above those of $Ni^{2+/3+}$ and $Co^{3+/4+}$. Therefore, the Mn^{4+} ions with a higher charge might not be able to move as easily as the other cationic species in the lattice. The Co³⁺ ions may not also move due to its larger OSSE. Therefore, only the lithium and nickel ions were found be mobile due to their lower charges and smaller OSSE. Moreover, lithium ions have no OSSE and encounter smaller electrostatic repulsion, as compared to the nickel ions. Therefore, lithium ions were found to have much higher tendency to move as compared to the nickel ions (Figure 5). Among the investigated samples, Li_{0.5}Ni_{0.35}Mn_{0.3}Co_{0.35}O₂ had the highest percentage change for both lithium ions (52%) from 3a site into 6c site, and nickel ions (27%) from 3b site into 3a site, as shown in Figure 5.

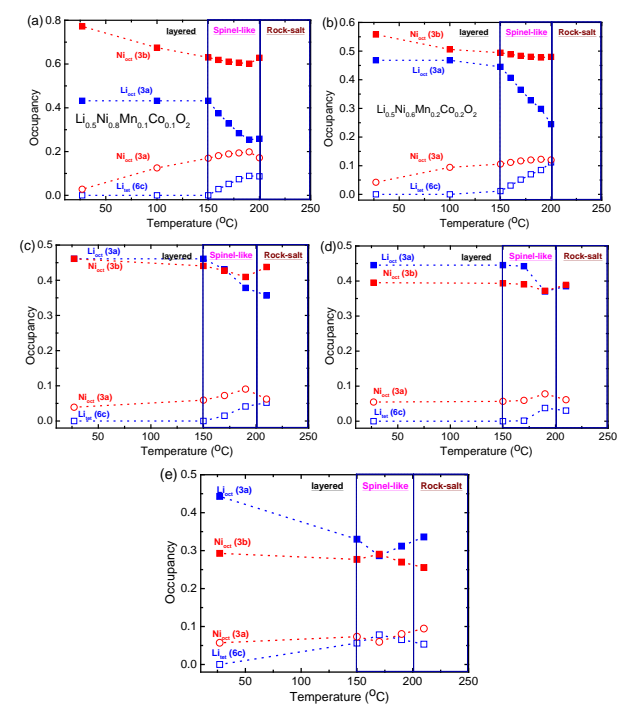


Figure 4. Change in the occupancy of Ni (3a, 3b) and Li (3a, 6c) in (a) $\text{Li}_{0.5}\text{Ni}_{0.8}\text{Mn}_{0.1}\text{Co}_{0.1}\text{O}_2$, (b) $\text{Li}_{0.5}\text{Ni}_{0.6}\text{Mn}_{0.2}\text{Co}_{0.2}\text{O}_2$, (c) $\text{Li}_{0.5}\text{Ni}_{0.5}\text{Co}_{0.5}\text{O}_2$, (d) $\text{Li}_{0.5}\text{Ni}_{0.45}\text{Mn}_{0.1}\text{Co}_{0.45}\text{O}_2$, and (e) $\text{Li}_{0.5}\text{Ni}_{0.35}\text{Mn}_{0.3}\text{Co}_{0.35}\text{O}_2$, as a function of temperature.

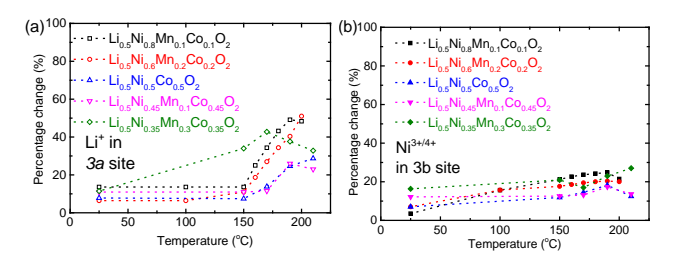


Figure 5. Percentage change in the occupancy of Li (3a) and Ni (3b) sites as a function of temperature for all the investigated samples.

As the spinel-like phases started to emerge at as low as 150 °C, all neutron diffraction patterns were also modeled with the spinel-type space group Fd-3m to understand the change in cell parameters as a function of temperature. In the fitting, anti-sites in spinel were also considered by allowing the transition-metal ions (Ni, Mn, Co; 16c site of Fd-3m) to partially occupy the lithium sites (8b site), or vice versa. For the first time, the cell parameter of the spinel-like species for Li-Ni-Mn-Co-O system was found to be 7.9 - 8.1 Å, in good agreement with other normal spinel-type lithium metal oxides.²¹ In general, a linear increase in the cell parameter with temperature was observed, and it suggested that some of the transitionmetal ions were partially reduced as the temperature increased. For the current study, about 15-20 mol.% of anti-site defect was found in the investigated samples (Figure 6f). The results pose some challenges that ideal and defect-free spinels are difficult to obtain for the Li-Ni-Mn-Co-O system, by the low temperature synthesis. Lastly, low defect samples are yet to be prepared by optimizing the experimental conditions.

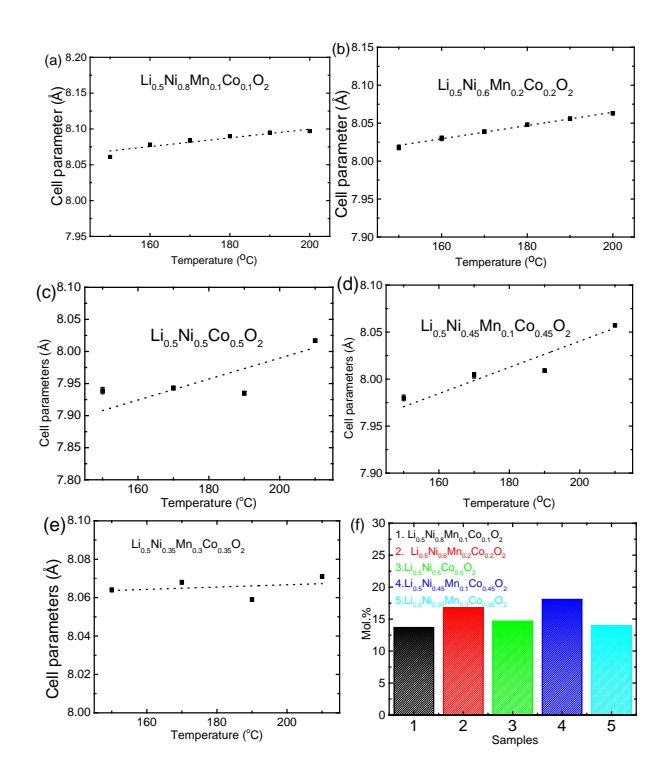


Figure 6. Cell parameters of the spinel-like (a) $\text{LiNi}_{1.6}\text{Mn}_{0.2}\text{Co}_{0.2}\text{O}_4$, (b) $\text{LiNi}_{1.2}\text{Mn}_{0.4}\text{Co}_{0.4}\text{O}_4$, (c) LiNiCoO_4 , (d) $\text{LiNi}_{0.9}\text{Mn}_{0.2}\text{Co}_{0.9}\text{O}_4$, and (e) $\text{LiNi}_{0.7}\text{Mn}_{0.6}\text{Co}_{0.7}\text{O}_4$ as a function of heat-treatment temperature. (f) Concentration (mol.%) of anti-site defects in the spinel-like samples.

3.2 Bond valence sum (BVS) map analysis. BVS map is often used to calculate the monovalent or divalent species (e.g., Li⁺, Na⁺, O²⁻) in ionic conductors.^{24, 33-34} Herein, BVS calculation was used to understand the ionic diffusion of both lithium and nickel ions during the transformation reaction. First of all, a hypothetical crystal information file (cif) of Li_{0.5}NiO₂ was created such that half of the lithium ions were distributed into the 3a sites, and the other half were located in the 6c sites. This atomic arrangement was to mimic the very first moment of the phase-conversion reaction. Quite interestingly, the lithium ions in 6c sites did not alter the 2D diffusion pathway in between the MO₂ slabs, as shown in Figure 7a, that the low bond valence (b.v. = 0.4) mismatch iso-surface overlaps well with the 3a and 6c sites. However, such a 2D iso-surface disappeared when a small amount (10%) of Ni ions was located in the 3a sites, indicating that the transport of lithium ions is highly impeded by Ni ions in the conduction plane. To understand if diffusion of lithium ions was necessary for the nickel ions to diffuse, another hypothetical cif file was created in which all lithium ions were located in the 6c sites and the bond valence sum map of Ni3+ ions was calculated. This was similar to the final stage of phase transformation. Ouite interestingly, another 2D iso-surface (b.v. = 0.05) for Ni³⁺ ions was revealed in Figure 7b. The overall calculation results support that diffusion of lithium ions should occur first in order to provide a low energy pathway for nickel ions to diffuse from 3b sites into 3a sites. On the basis of the neutron diffraction analysis, only lithium and nickel ions were found to move as the temperature increased. Therefore, it is challenging to complete the phase conversion for samples with low nickel content as other transition-metal ions would not participate in

the diffusion, and the nickel-ion movement was only favorable when most the lithium ions moved into 6c sites.

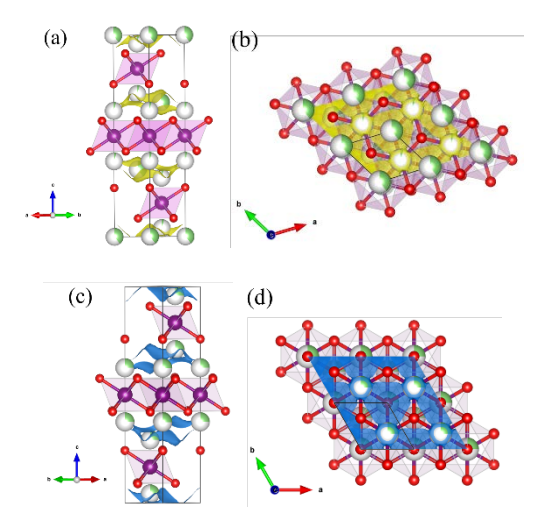


Figure 7. Bond valence sum (BVS) map of Li⁺ ions on (110) and (003) planes are shown in (a) and b), respectively, for layered-type (R-3m) Li $_{0.5}$ NiO $_2$. The corresponding BVS map of Ni³⁺ ions on (110) and (003) planes are also shown in (c) and (d), respectively.

3.3 Electrochemical performance of spinel-like samples.

The impact of ionic diffusion on the electrochemical performance was evaluated in a coin-cell configuration. Two repre- $Li_{0.5}Ni_{0.8}Mn_{0.1}Co_{0.1}O_{2} \\$ sentative samples, Li_{0.5}Ni_{0.6}Mn_{0.2}Co_{0.2}O₂, were chosen as they had substantially more ionic diffusion for lithium and/or nickel ions to represent the targeted spinel-like compounds. As shown in Figure 8, the slope-like characteristic of the layered-type structure was still clearly observed in the discharge profile of the samples heattreated at 150 °C for 12 h. Nonetheless, the ionic moment of lithium and/or nickel ions did impact strongly the discharge voltage and specific capacity, particularly heating at higher temperatures. Unlike the LiMn₂O₄ spinel, a second plateau was not observed at 2.5 - 3 V.3,35 This might be because the accessibility of such octahedral sites for the insertion of a second lithium is blocked by the transition-metal ions. When the temperature was increased further, more spinel and rock-salt phases were formed until about 200 °C. But the defective spinel-like and rock-salt species did not contribute positively to the capacity, and therefore specific capacity was found to decrease as the heating temperature increased. Finally, a better electrochemical performance may be possibly by optimizing the synthetic conditions and chemical composition.

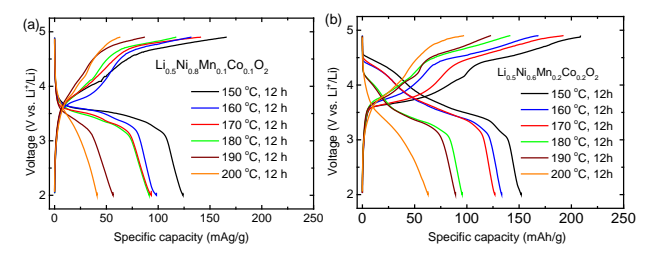


Figure 8. Charge-discharge profiles of the 2^{nd} cycle of (a) $Li_{0.5}Ni_{0.8}Mn_{0.1}Co_{0.1}O_2$ and (b) $Li_{0.5}Ni_{0.6}Mn_{0.2}Co_{0.2}O_2$ after heat-treating at 150-200 °C for 12 h.

4. CONCLUSION

A new metastable normal spinel-like phase diagram has been investigated for the Li-Ni-Mn-Co-O system by a low-temperature synthesis approach. Our study shows that a high yield for spinel-like phases and defect-free spinel phases are difficult to obtain, but further optimization in terms of synthesis conditions and chemical compositions could help improve the quality of the spinel-like phase by eliminating the defects and thereby boost the electrochemical performance. We anticipate that the methodology presented here could become useful to synthesize other complex spinel compounds from their layered-type counterparts.

ASSOCIATED CONTENT

Supporting Information. *Ex-situ* powder X-ray diffraction patterns for $\text{Li}_{0.5}\text{Ni}_{1-2y}\text{Mn}_y\text{Co}_y\text{O}_2$ ($y=0.1,\ 0.15,\ 0.2,\ 0.25$) and $\text{Li}_{0.5}\text{Ni}_{0.5-y}\text{Mn}_{2y}\text{Co}_{0.5-y}\text{O}_2$ ($y=0,\ 0.05,\ 0.1,\ 0.15$)

AUTHOR INFORMATION

Corresponding Author

* E-mail: manth@austin.utexas.edu.

ACKNOWLEDGMENT

This work was supported by the Welch Foundation grant F-1254. The neutron diffraction measurement at the POWGEN beamline at the Oak Ridge National Laboratory's (ORNL) Spallation Neutron Source (SNS) was sponsored by the Scientific User Facilities Division, Office of Basic Energy Sciences, US Department of Energy. The authors appreciate the technical help and useful discussion with Drs. Melanie Kirkham and Pamela Whitfield at the POWGEN in ORNL, and Dr. Bohang Song at the University of Texas at Austin. Use of the Advanced Photon Source at Argonne National Laboratory was supported by the U. S. Department of Energy, Office of Science, Office of Basic Energy Sciences, under Contract No. DE-AC02-06CH11357.

REFERENCES

- (1) Mizushima, K.; Jones, P. C.; Wiseman, P. J.; Goodenough, J. B., Lithium Cobalt Oxide(LixCoO2) (0<x≤1): A New Cathode Material for Batteries of High Energy Density. *Mater. Res. Bull.* **1980**, *15*, 783-9.
- (2) Thackeray, M. M.; David, W. I. F.; Bruce, P. G.; Goodenough, J. B., Lithium Insertion into Manganese Spinels. *Mater. Res. Bull.* **1983**, *18*, 461-72.
- (3) Thackeray, M. M.; Johnson, P. J.; De Picciotto, L. A.; Bruce, P. G.; Goodenough, J. B., Electrochemical Extraction of Lithium from Lithium Manganate (LiMn2O4). *Mater. Res. Bull.* **1984**, *19*, 179-87.
- (4) Goodenough, J. B.; Manthiram, A., A Perspective on Electrical Energy Storage. *MRS Commun.* **2014**, *4*, 135-142.
- (5) Manthiram, A., Materials Challenges and Opportunities of Lithium Ion Batteries. *J. Phys. Chem. Lett.* **2011**, *2*, 176-184.
- (6) Manthiram, A.; Chemelewski, K.; Lee, E.-S., A Perspective on the High-Voltage Limn1.5ni0.5o4 Spinel Cathode for Lithium-Ion Batteries. *Energy Environ. Sci.* **2014**, *7*, 1339-1350.
- (7) Padhi, A. K.; Nanjundaswamy, K. S.; Goodenough, J. B., Phospho-Olivines as Positive-Electrode Materials for Rechargeable Lithium Batteries. *J. Electrochem. Soc.* **1997**, *144*, 1188-1194.
- (8) Padhi, A. K.; Nanjundaswamy, K. S.; Masquelier, C.; Okada, S.; Goodenough, J. B., Effect of Structure on the Fe3+/Fe2+ Redox Couple in Iron Phosphates. *J. Electrochem. Soc.* **1997**, *144*, 1609-1613.
- (9) Nazri, G.-A.; Pistoia, G.; Editors, *Lithium Batteries: Science and Technology*; Kluwer Academic Publishers, 2004, p 708 pp.

- (10) Takami, N.; Inagaki, H.; Tatebayashi, Y.; Saruwatari, H.; Honda, K.; Egusa, S., High-Power and Long-Life Lithium-Ion Batteries Using Lithium Titanium Oxide Anode for Automotive and Stationary Power Applications. *J. Power Sources* **2013**, 244, 469-475.
- (11) Belharouak, I.; Koenig, G. M., Jr.; Amine, K., Electrochemistry and Safety of Li4Ti5O12 and Graphite Anodes Paired with Limn2o4 for Hybrid Electric Vehicle Li-Ion Battery Applications. *J. Power Sources* **2011**, *196*, 10344-10350.
- (12) Sigala, C.; Guyomard, D.; Verbaere, A.; Piffard, Y.; Tournoux, M., Positive Electrode Materials with High Operating Voltage for Lithium Batteries: LiCryMn2-YO4 ($0 \le Y \le 1$). Solid State Ionics **1995**, 81, 167-70.
- (13) Tarascon, J. M.; Wang, E.; Shokoohi, F. K.; McKinnon, W. R.; Colson, S., The Spinel Phase of Lithium Manganese Oxide (LiMn2O4) as a Cathode in Secondary Lithium Cells. *J. Electrochem. Soc.* **1991**, *138*, 2859-64.
- (14) Gummow, R. J.; de Kock, A.; Thackeray, M. M., Improved Capacity Retention in Rechargeable 4 V Lithium/Lithium Manganese Oxide (Spinel) Cells. *Solid State Ionics* **1994**, *69*, 59-67.
- (15) Zhong, Q.; Banakdarpour, A.; Zhang, M.; Gao, Y.; Dahn, J. R., Synthesis and Electrochemistry of Linixmn2-Xo4. *J. Electrochem. Soc.* **1997**, *144*, 205-213.
- (16) Choi, J.; Manthiram, A., Role of Chemical and Structural Stabilities on the Electrochemical Properties of Layered LiNi1/3Mn1/3Co1/3O2 Cathodes. *J. Electrochem. Soc.* **2005**, *152*, A1714-A1718.
- (17) Li, D.; Kato, Y.; Kobayakawa, K.; Noguchi, H.; Sato, Y., Preparation and Electrochemical Characteristics of LiNi1/3Mn1/3Co1/3O2 Coated with a Metal Oxide Coating. *J. Power Sources* **2006**, *160*, 1342-1348.
- (18) Li, D.-C.; Muta, T.; Zhang, L.-Q.; Yoshio, M.; Noguchi, H., Effect of Synthesis Method on the Electrochemical Performance of LiNi1/3Mn1/3Co1/3O2. *J. Power Sources* **2004**, *132*, 150-155.
- (19) Rao, C. V.; Reddy, A. L. M.; Ishikawa, Y.; Ajayan, P. M., LiNi1/3Co1/3Mn1/3O2-Graphene Composite as a Promising Cathode for Lithium-Ion Batteries. *ACS Appl. Mater. Interfaces* **2011**, *3*, 2966-2072
- (20) Riley, L. A.; Van Atta, S.; Cavanagh, A. S.; Yan, Y.; George, S. M.; Liu, P.; Dillon, A. C.; Lee, S.-H., Electrochemical Effects of Ald Surface Modification on Combustion Synthesized LiNi1/3Mn1/3Co1/3O2 as a Layered-Cathode Material. *J. Power Sources* **2011**, *196*, 3317-3324.
- (21) Villars, P.; Cenzual, K., Pearson's Crystal Data: Crystal Structure Database for Inorganic Compounds (on Dvd), Release 2015/16, Asm International®, Materials Park, Ohio, USA. 2015.
- (22) Brown, C. R.; McCalla, E.; Watson, C.; Dahn, J. R., Combinatorial Study of the Li-Ni-Mn-Co Oxide Pseudoquaternary

- System for Use in Li-Ion Battery Materials Research. *ACS Comb. Sci.* **2015**, *17*, 381-391.
- (23) Shukla, A. K.; Ramasse, Q. M.; Ophus, C.; Duncan, H.; Hage, F.; Chen, G., Unravelling Structural Ambiguities in Lithium- and Manganese-Rich Transition Metal Oxides. *Nat. Commun.* **2015**, *6*, 8711
- (24) Kan, W. H.; Huq, A.; Manthiram, A., Low-Temperature Synthesis, Structural Characterization, and Electrochemistry of Ni-Rich Spinel-Like LiNi2-YMnyO4 ($0.4 \le Y \le 1$). *Chem. Mater.* **2015**, Ahead of Print.
- (25) Toby, B. H., Expgui, a Graphical User Interface for Gsas. *J. Appl. Crystallogr.* **2001**, *34*, 210-213.
- (26) Sale, M.; Avdeev, M., 3dbvsmapper: A Program for Automatically Generating Bond-Valence Sum Landscapes. *J. Appl. Crystallogr.* **2012**, *45*, 1054-1056.
- (27) Zheng, J.; Kan, W. H.; Manthiram, A., Role of Mn Content on the Electrochemical Properties of Nickel-Rich Layered LiNi0.8-xCo0.1Mn0.1+xO2 ($0.0 \le x \le 0.08$) Cathodes for Lithium-Ion Batteries. *ACS Appl. Mater. Interfaces* **2015**, 7, 6926-6934.
- (28) Arai, H.; Sakurai, Y., Characteristics of Lixnio Obtained by Chemical Delithiation. *J. Power Sources* **1999**, *81*-82, 401-405.
- (29) Arai, H.; Tsuda, M.; Saito, K.; Hayashi, M.; Takei, K.; Sakurai, Y., Structural and Thermal Characteristics of Nickel Dioxide Derived from LiNiO2. *J. Solid State Chem.* **2002**, *163*, 340-349.
- (30) Dahn, J. R.; Fuller, E. W.; Obrovac, M.; von Sacken, U., Thermal Stability of LixCoO2, LixNiO2 and Λ-Mno2 and Consequences for the Safety of Li-Ion Cells. *Solid State Ionics* **1994**, *69*, 265-70.
- (31) Armstrong, A. R.; Bruce, P. G., Synthesis of Layered LiMnO2 as an Electrode for Rechargeable Lithium Batteries. *Nature (London)* **1996**, *381*, 499-500.
- (32) Choi, S.; Manthiram, A., Factors Influencing the Layered to Spinel-Like Phase Transition in Layered Oxide Cathodes. *J. Electrochem. Soc.* **2002**, *149*, A1157-A1163.
- (33) Kan, W. H.; Huq, A.; Manthiram, A., The First Fe-Based Na+-Ion Cathode with Two Distinct Types of Polyanions: Fe3P5SiO19. *Chem. Commun. (Cambridge, U. K.)* **2015**, *51*, 10447-10450.
- (34) Adams, S., Lithium Ion Pathways in Lifepo4 and Related Olivines. *J. Solid State Electrochem.* **2010**, *14*, 1787-1792.
- (35) Thackeray, M. M.; Shao-Horn, Y.; Kahaian, A. J.; Kepler, K. D.; Skinner, E.; Vaughey, J. T.; Hackney, S. A., Structural Fatigue in Spinel Electrodes in High Voltage (4 V) Li/LixMn2O4 Cells. *Electrochem. Solid-State Lett.* **1998**, *1*, 7-9.

Table of Contents

